ARMA 10-239

Geomechanics applied to the well design through salt layers in Brazil: A History of success

Costa, A.M.; Poiate Jr, E.; Amaral, C.S.; Gonçalves, C.J.C and Falcão, J.L.
PETROBRAS Petróleo Brasileiro S.A., Rio de Janeiro, Rio de Janeiro, Brazil
Pereira, A.
Pontifical Catholic University of Rio de Janeiro, Rio de Janeiro, Rio de Janeiro, Brazil

This paper was prepared for presentation at the 44th US Rock Mechanics Symposium and 5th U.S.-Canada Rock Mechanics Symposium, held in Salt Lake City, UT June 27–30, 2010.

ABSTRACT: A major challenge in drilling in the Pre-salt area, in Brazil, arises from the special structural salt behavior, when compared to other geomaterials, since it develops high creep strain rates under high levels of deviatoric stresses and temperatures. The salt or evaporitic rocks, formed by the sea water evaporation, have different chemical compositions. In the Pre-salt area the more important types are: halite, carnallite and tachyhydrite. The tachyhydrite, for the same state variables, deviatoric stress and temperature, develops creep strain rates up to one hundred times higher than halite. Many operational problems, such as stuck pipe and casing collapse, have been reported when intercalation of these rocks within a thick layer is found. The challenge of designing excavations near tachyhydrite, began with the development of an underground mine to extract sylvinite ore in Northeast Brazil. The research that began in the 70s, to enable the mining of this ore overlying this rock, triggered one of the largest R&D projects in rock mechanics, including computing modeling, laboratory and field tests. For the design of the pre-salt wells this previous experience was used and additional triaxial creep tests were performed using a new rock mechanics laboratory. Field tests and computer modeling improvement were used to overcome the challenge of the Pre-salt drilling. This article describes the lessons learned on the geomechanical salt behavior and its application in subsalt wells design. In addition, it is presented the developed methodology validation, through comparison between computing modeling results with measurements carried out in experimental panels, in the potash mine, and with measurements obtained in an experimental well drilled for the purpose of calibrating and optimizing directional drilling in salt layers. These parameters and methodology have been used to support the design of the wells drilled in the Pre-Salt giant oil fields in Brazil with very successful results.

1. INTRODUCTION

Rock mechanics applied to salt rock started in Brazil with the discovery of potash reserves, sylvinite ore (NaCl.KCl) in the State of Sergipe, during oil exploration by PETROBRAS in the 1960s. The sylvinite ore body is located at the depth varying from 450m to 640m from surface. This reserve can be, in a simplified way, divided in two layers, the upper sylvinite and the lower sylvinite separated by a halite layer, Fig.1.

In some regions of the reserve, the lower sylvinite overlies the rock tachyhydrite ($CaCl_2 \cdot 2MgCl_2 \cdot 12H_2O$), which is very weak in comparison to halite and can develop creep strain rate, two orders of magnitude faster than halite, for the same state variables, temperature and stress. Due to this geotechnical challenge it was decided to start the development of the mine by the upper sylvinite and the mining basic project of the lower sylvinite would be done after an extensive research of rock mechanics, including laboratory and field tests and computer modeling [17].

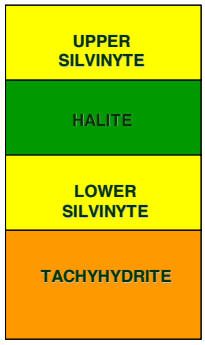

Fig. 1. Typical geology section of the potash reserve in the state of Sergipe in Brazil

The shaft excavation of the mine started in the early 1980s. Due to the very successful rock mechanics research done, the upper and the lower sylvinite layers are currently being mined. All this background experience on the mechanical behavior of these types of evaporites, found in the potash mine, has been used in the designing of the wells for oil exploration in Santos Basin by Petrobras.

The Santos Basin, offshore southeast Brazil, is one of the Brazilian basins that is receiving considerable industry attention nowadays, with the discovery of the giant oil fields known as Pre-Salt reservoirs.

The Pre-Salt reservoirs in Santos basin are located in water depth varying from 150m up to 2200m. To reach the Pre-Salt reservoirs located in deep water it is necessary to drill through 2000m of salt rock, mainly halite, and in some places, tachyhydrite ($CaCl_2 \cdot 2MgCl_2 \cdot 12H_2O$), and carnallite ($KCl \cdot MgCl_2 \cdot 6H_2O$) intercalations are found. The rock mechanics research program developed to overcome this new challenge of drilling through very thick salt rock layers is an extension of the research done for the lower sylvinite layer of the potash mine in the state of Sergipe.

2. CONSTITUTIVE EQUATION FOR SALT BEHAVIOR

Due to its crystalline structure, salt rocks exhibit time-dependent behavior when subjected to shear stress. The creep strain rate is influenced by the formation temperature, mineralogical composition, water content, presence of impurities, and the extent to which differential stresses are applied to the salt body. Chloride and sulphate salts containing water (bischofite, carnallite, kieserite and tachyhydrite) are the most mobile. Halite is relatively slow-moving, and anhydrite and the carbonates (calcite, dolomite) are essentially immobile [5].

Early in the 1990´s, creep constitutive laws based on deformation mechanisms, have been recommended by the international technical literature, to represent the intrinsic behavior of the evaporates [7-9].

The law that incorporates the deformation mechanisms for the evaporite rocks was developed by Munson [7,8]. The constitutive equation based on Munson's creep law considers the following mechanisms: Dislocation Glide, Dislocation Climb and Undefined Mechanism. The largest contribution of either mechanism depends on the temperature conditions and differential stress to which the salt is submitted.

The constitutive equation corresponding to the creep law of double deformation mechanism is a simplification of the equation developed by Munson, and it considers the creep mechanisms Dislocation Glide and Undefined Mechanism.

The latter effect was recently identified as being creep in the contacts of the salt grains, provoked by the dissolution of the salt in function of the increase of its solubility under the high pressures that happen in the contacts among grains.

In this paper, halite is analyzed according to the elasto/visco-elastic behavior, adopting the Double Mechanism creep law, as shown in equation 1:

$$\varepsilon = \varepsilon_0 \cdot \left(\frac{\sigma_{ef}}{\sigma_0} \right)^n . e^{\left(\frac{Q}{RT_0} - \frac{Q}{RT} \right)} \quad (1)$$

where

ε – Strain rate due to creep at the steady state condition
ε_0 – Reference strain rate due to creep (in steady state)
ε_{ef} – Creep effective stress
ε_0 – Reference effective stress
Q – Activation energy (kcal/mol), Q=12 kcal/mol [8]
R – Universal gas constant (kcal/mol.K), R=1.9858E-03
T_0 – Reference temperature (K)
T – Rock temperature (K)

3. SALT SAMPLES

All of salt samples were obtained from wells located in the Northeast of Brazil (Sergipe State). The samples are stored in a temperature and humidity controlled room, to preserve the specimens, due to the hygroscopic behavior of the evaporites. Figure 2 shows the samples obtained from oil exploration wells drilled in Sergipe.

(a) (b) (c)

Fig. 2. Samples used for rock mechanics tests: (a) Halite; (b) Carnallite; (c) Tachyhydrite

As a consequence of the sampling process, cracks could be induced in the sample, which could affect its mechanical behavior. Those cracks and the larger or smaller presence of insolubles, such as clay and interbedded shale and anhydrite reduce the compressional velocity. To prevent this effect, the samples were prepared (top and bottom are grounded)

and submitted to a quality control to verify their structural integrity through the measurement of compressional velocity (PUNDIT instrument). For example, halite samples with compressional velocity below 4300m/s were rejected.

The porosity of the halite is negligible, its permeability being lower than 1μD, which turns the compressional velocity a constant mechanical property regardless of the depth. This fact can be observed in the sonic profile of an exploratory well that crosses thick layers of pure halite.

The samples were used in the creep tests in order to determine the creep constants required for the double mechanism creep law. The elastic constants, Young Modulus and Poisson ratio were obtained by measurements of compressional and shear velocity in the potash mine through the application of direct reflection seismic [22] on the floor and on the pillar faces in the mine. These constants have been used for decades to design the room and pillar structures of the mine. The Dynamic Young Modulus can be obtained by using the elasticity theory. Applying the Dynamic Poisson's Ratio of 0.36, which value has been used in several works related with the mechanical behavior of the salt in the potash mine of Taquari-Vassouras - Northeast of Brazil, determined, and presented in the international technical literature.

The creep tests were performed in specimens with a length/diameter ratio of 2 (ISRM Standards) in a Laboratory of Rock Mechanics and Rock Hydraulics from IPT - Institute for Technological Research of the State of São Paulo – Brazil [14,15].

4. EXPERIMENTAL ASSEMBLY

A laboratory with six independent creep test stations was built in IPT [14,15]. Each station uses an automatic servo control system, keeping the confining pressure and the axial pressure constant during the test.

The units consist of a hydraulic and pneumatic servo control system, electrical resistance, stove, and measurement instruments like LVDT´s, pressure transducers and thermocouples. All instruments are connected to a data acquisition system MGC Plus (HBM), connected to the computer, which is controlled by a code specially written in CatMan program (HBM). The computer code controls the test and can plot in real time the temperature, confined pressure, axial load and axial deformation and store all the information in a database.

Specimen axial strain is measured with time sampling of 1s, while the confining pressure, differential stress, and temperature are held constant for the duration of the test.

Due to the long time necessary to complete a creep test, to guarantee its quality, without the influence of energy fluctuation and interruption, no-breaks and energy generator were installed.

After completion the experimental assembly the confining pressure is applied, followed by the temperature and finally the axial pressure, inducing the differential stress to the specimen. Figure 3 illustrates one of the creep test stations in the IPT lab.

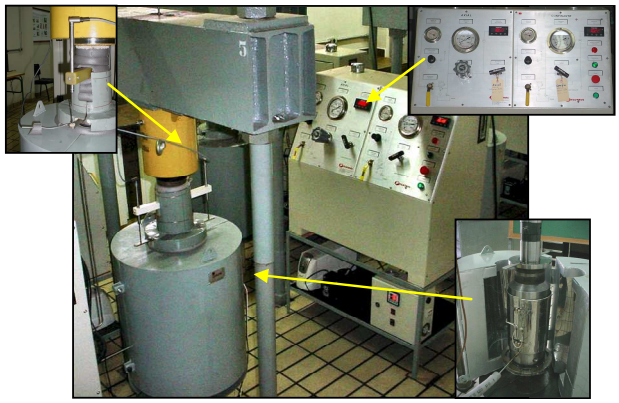

Fig. 3. Final assembling of the testing apparatus and Hydraulic control system.

5. CREEP TESTING RESULTS

A typical axial creep deformation curve is illustrated in Figure 4.

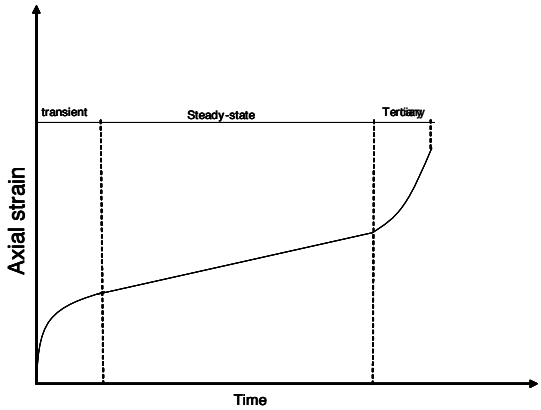

Fig. 4. Creep testing result from a salt rock specimen: all possible stages.

Three important stages of the salt rock creep behavior must be handled appropriately when material model parameters are evaluated in the laboratory.

A typical creep curve for salt consists of two or three creep stages. Following the application of the stress difference, the strain rate is very high. This rate then decreases monotonically with time until a constant strain rate is observed. These two stages are called transient and steady state creep stages, respectively. Depending on

the level of temperature and the differential stress applied to the specimen a third stage, called tertiary creep, may become evident. This is characterized by acceleration of the creep strain rate caused by the specimen structure damage induced by the creep strain accumulation with time. At the tertiary creep stage the dilation phenomenon, an increase in volume through micro fracturing develops, leading to failure of the specimen.

Figure 5 shows a typical salt creep rock behavior. In these tests, tachyhydrite, carnallite and halite are submitted to a 10MPa differential stress and 86ºC temperature. In 160 hours testing time, the specific accumulated axial strains are 15%, 5.50% and 0.14% for tachyhydrite, carnalite and halite respectively. With these test parameters, tachyhydrite creeps approximately 107 times faster than halite and 2.7 times faster than carnallite [26, 27].

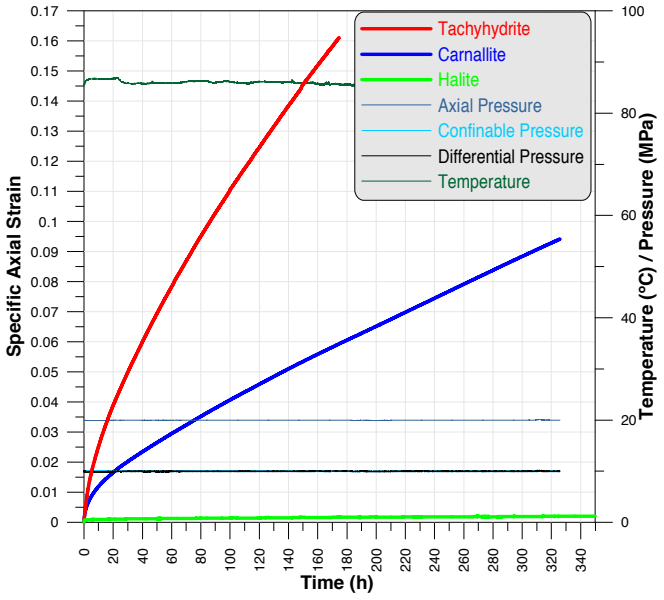

Fig. 5. Salts creep test, 86ºC, Δσ=10MPa.

The double mechanism constitutive creep equation in (1) represents only the steady-state creep stage. The transient creep, for the conditions normally found in mining and oil well drilling, is fully dissipated in a short period of time and can be absorbed by the initial deformation predicted by the numerical models. To obtain the constants ε_0, σ_0 and n, it is necessary to establish the relation between the steady-state creep strain rate and the differential stress applied to the specimen for a specific temperature.

Figure 6 shows a typical behavior of salt creep. In this test, halite is submitted to a 16MPa differential stress and 86ºC temperature [14]. The first stage, transient creep, is observed up to 200h. Between 200h and 1600h, steady-state creep is observed, with strain rate of 7.7673E-05/hour. After 1700h, the tertiary creep is observed. The differential pressure of 16MPa is about 45% of the rupture stress of the sample, obtained by the simple compression test.

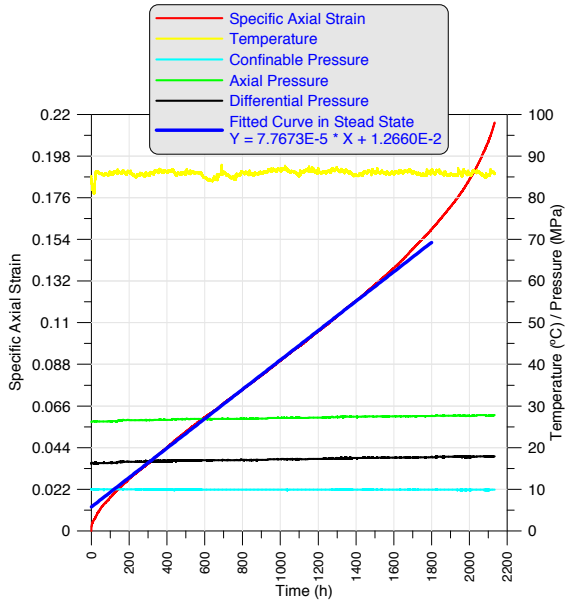

Fig. 6. Halite creep curve (Temperature of 86ºC and differential stress of 16MPa).

Fig. 8 Shows the steady-state creep strain rate for different differential stresses, ranging from 6-20MPa, in di-log scale.

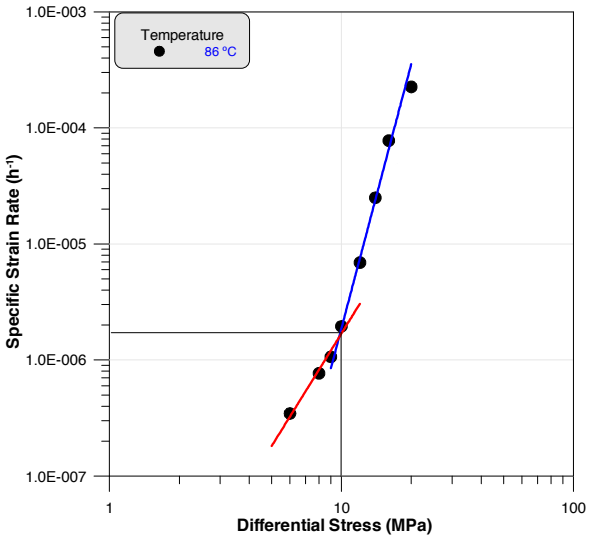

Fig. 8. Steady-state creep strain rate x differential stress for halite (Temperature 86ºC).

From the interpolation, in di-log scale, the values of σ_0 and ε_0 can be determined for the test temperature, 86ºC:
$(X , Y) = (9.91 , 1.880E\text{-}06) = (\sigma_0 , \varepsilon_0)$
$\sigma_0 = 9.91 \cong 10MPa$

Therefore, the Constitutive Equation becomes:
$\varepsilon = 1.880E\text{-}06\ (\sigma_{ef} / 10)^n$

In which:

$n = 3.36 \rightarrow \sigma_{ef} < \sigma_0$
$n = 7.55 \rightarrow \sigma_{ef} \geq \sigma_0$

The same procedure is used for carnallite and tachyhydrite to obtain the creep parameters.

Figure 8 shows the result of a creep test on a halite specimen when a confining pressure of 10MPa, differential stress of 10MPa and temperature of 130°C are applied.

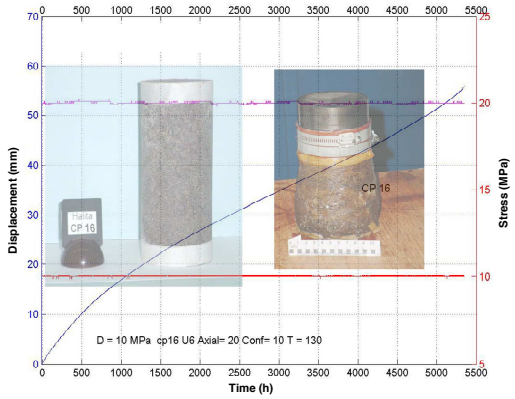

Fig. 8. Creep Test on halite ($\Delta\sigma$ = 10MPa, T=130°C).

6. VALIDATION OF THE CREEP PARAMETERS

6.1. *Comparison with closure measurements from the potash mine*

As part of the rock mechanics studies, used to enable the mining of the lower sylvinite layer in the potash mine, an experimental panel, "D1" [20,24,28,29] was designed and excavated in the lower sylvinite layer, overlying a layer of tachyhydrite 15m thick. An experimental room, "C1D1", was excavated in this panel isolated from the effects of nearby excavations, with intensive use of field instrumentation, for back-analysis, allowing the calibration of the creep parameters. Figure 9 shows the layout of the mine and the location of the experimental panel D1 and the experimental room C1D1.

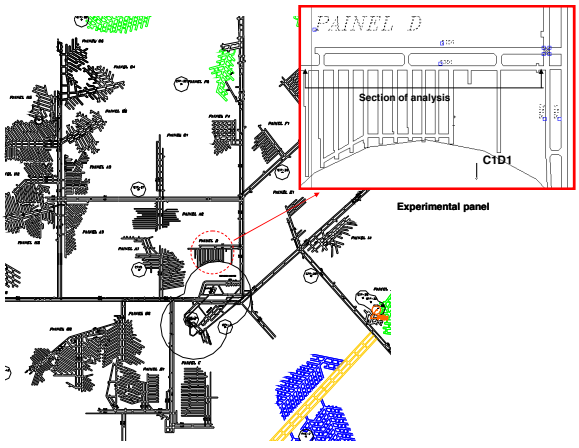

Fig. 9. Experimental panel D1 and experimental room C1D1.

The experimental room C1D1 was designed and excavated with length of 95m, divided in three sections. In each section a slab protection was left, with three different thickness, 3m, 2m and 1m. The strategy is to evaluate the influence of the slab protection thickness of sylvinite in inhibiting the floor heave due to the creep of tachyhydrite. Among the various instruments installed in the room, this paper shows the comparison between the vertical closure measurements with those obtained by the numerical simulation. Figure 10 shows a typical vertical closure measurement section used in the mine.

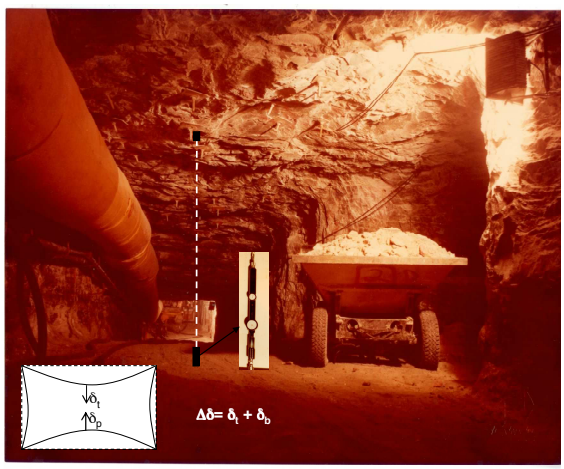

Fig. 10. Typical closure measurement section in the mine.

The geology description in the area of the experimental panel D1 is show in Figure 11.

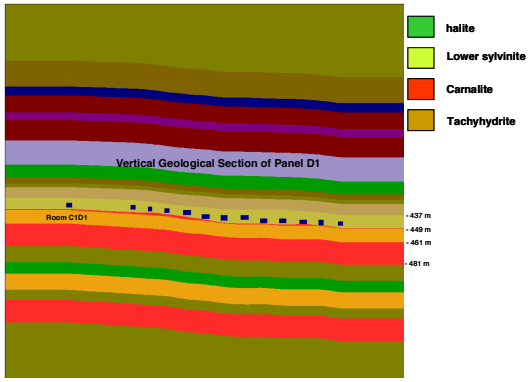

Fig. 11. Geology description in the experimental panel.

For comparison, a plain strain model is used through a vertical geology section as indicated in Figure 11. Figure 12 shows the finite element model used in the simulations.

The SIGMA [16] system is used for pre and post processing of the finite element model. The numerical simulations have been done through application of the finite element code ANVEC [17]. The ANVEC program is extensively applied in the behavior simulation of the underground excavations [17-21], considers the non-linear physical elasto/visco-elastic phenomenon, with constitutive law of double mechanism of deformation by

creep. The program has shown excellent stability and convergence to predict the creep phenomenon in conditions of high temperature levels and high differential stresses and the procedure of simulating the behavior of the well with time as a function of the bit progress, through the technique of automatic mesh rezoning. This constituted in a differential advantage of the program providing valuable inputs for the drilling operation [10, 11, 14, 15].

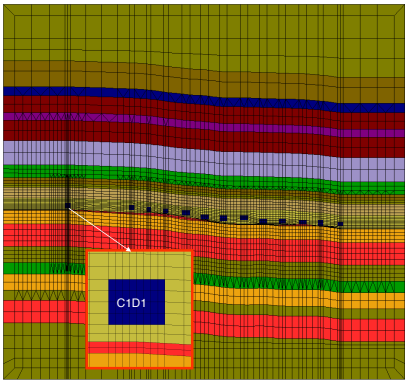

Fig. 12. Finite element model of the experimental room C1D1.

Figures 13 and 14 show the comparison between the closure measured in the experimental gallery in different locations along its axis for different thickness of the sylvinite slab protection. Each plot shows the closure predicted by numerical simulation with and without the initial deformation after excavation, which normally is lost in the field. In these numerical models it is used the creep parameters obtained in the laboratory creep tests.

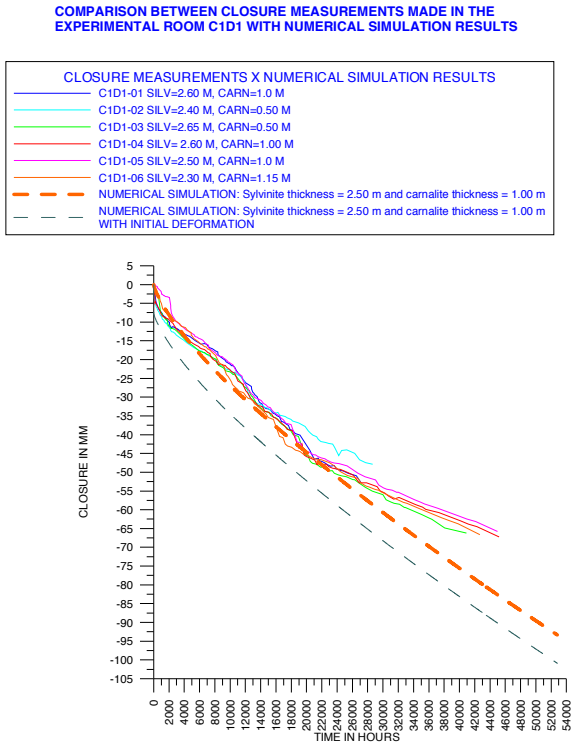

Fig. 13. Comparison between closure measurements and numerical simulation, sylvinite slab protection 2.5m thick.

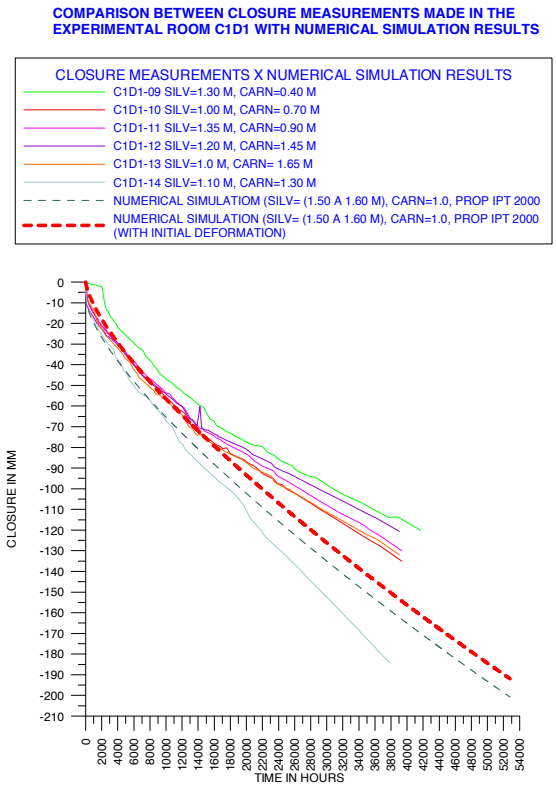

Fig. 14. Comparison between closure measurements and numerical simulation, sylvinite slab protection 1.0-1.3m thick.

The results obtained by numerical simulation shows excellent fit to the closure measured in the experimental room C1D1 up to 16000h. After this time the refrigeration process starts in the mine and reduces the rock temperature and the creep measurements. This process wasn't introduced in the numerical simulation. This way the first step in the validation process of the creep parameters was performed.

The constitutive creep equation and creep parameters were also validated by comparison with closure measurements by caliper in an experimental directional well drilled in an oil field in the same evaporitic basin of the potash reserve in the state of Sergipe. Again very good fit was obtained between both results, numerical and caliper measurements.

6.2. 2D model versus 3D model

In order to validate the 3D model 2D (axisymmetric) model was built, according to the longitudinal axis of the wellbore diameter of 8 ½" and comprises 19.25m of salts interval and the radius model of 25m (to avoid boundary condition problems). 440 quadratic isoparametric elements (with 8 nodes) and 1423 nodal points were employed in the finite element model, shown in Fig. 15. To consider the temperature variation in depth, and the lithology, different layers were built.

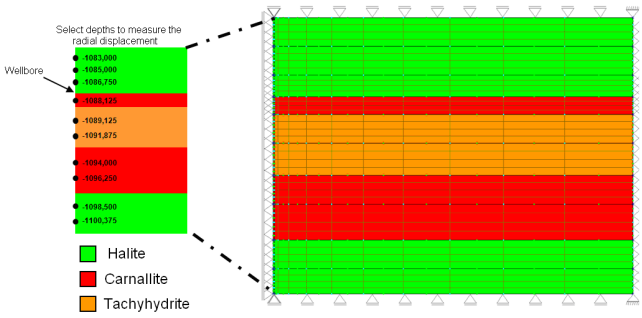

Fig. 15. 2D model.

The 3D model was performed at the same depth (-1082m to -1101.25m) and with the same layers of the 2D model. 7680 quadratic hexaedric elements (with 20 nodes) and 34061 nodal points were employed in the finite element model, shown in Fig. 16. To consider the temperature variation in depth, and the lithology, different layers were built.

The wellbore radial closure with 7.5lb/gl mud weight in the selects depths from 2D and 3D model are present in the Fig. 17. The matches range from good to excellent.

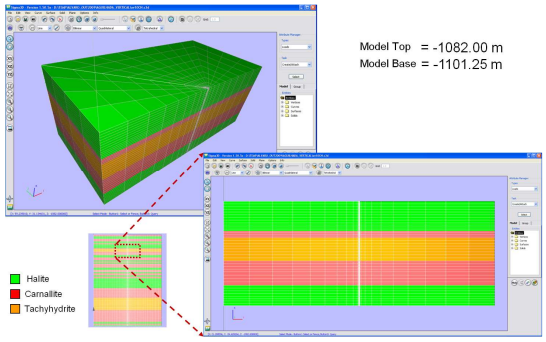

Fig. 16. 3D model.

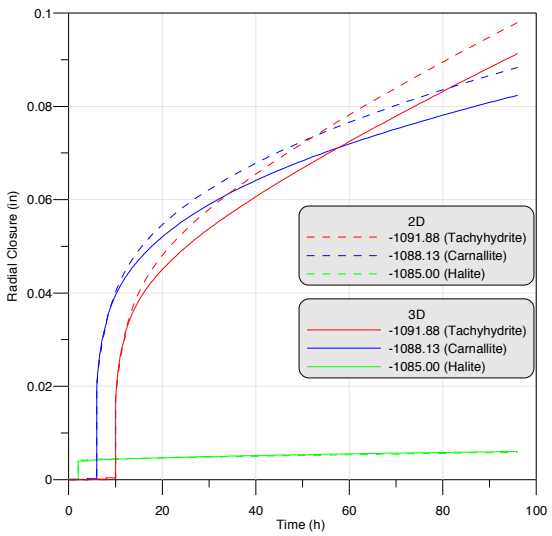

Fig. 17. The 2D and 3D results from the radial closure.

6.3. Experimental well

An additional test (i.e., an experimental directional well drilling) has been performed in the evaporític basin of Sergipe State in order to give support to directional drilling in thick layers of salt at the Santos Basin. For comparisons with the experimental results, a 3D model is generated through the complete vertical geology section indicated in Figure 18.

The finite element model used in the well simulations is shown in Figure 18. The SIGMA system [16] was also used to create the model and to post process the results, whereas the numerical simulations were performed in the ANVEC [17] 3D package.

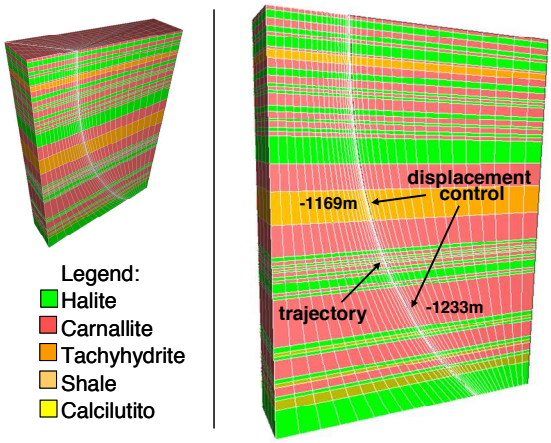

Fig. 18. 3D finite element model of the experimental well.

Several simulations were performed (e.g. considering different fluid weights, anisotropy states, etc) in order to compare with the results obtained in the experimental well. Two plots of closure predicted by numerical simulation are shown in Figure 19. These plots refer to two different locations along the model vertical axis (model depth). In these numerical models, it is used the creep parameters obtained in the laboratory creep tests.

The results obtained by the numerical simulations show excellent fit to the closure measured in the experimental drilling, which is crucial to certify the validation process of the creep parameters.

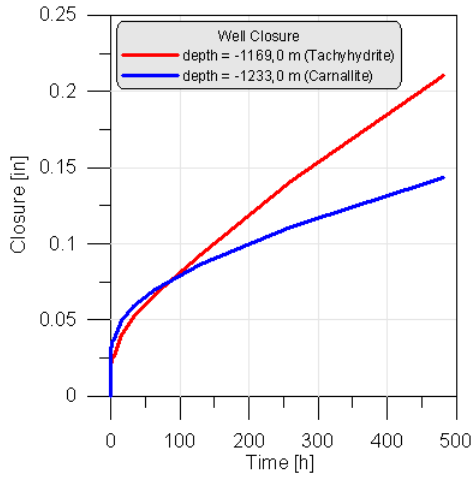

Fig. 19. Closures predicted by numerical simulation for two different depths.

The results obtained in the 3D well simulations reinforce the capabilities and the differential advantage of the ANVEC program in providing valuable subsidies for the drilling operations.

7. FINITE ELEMENT MODEL OF WELL CLOSURE

With the creep parameters validation, it was applied the constitutive equation in the numerical simulation of the creep salt behavior to predict the evolution of well closure with time during drilling of thick layers of salt, for various mud weights. These results were used to define several technically feasible alternatives for the drilling strategy through the salts intervals. This paper shows two case studies analyzed by this methodology.

7.1. Case Study 1

The prospect expected 2000m of different salt rocks, to be drilled at the interval of 2600 to 4600m, (WD = 1600m), Figure 20. This case study considered a tachyhydrite layer of 5m just 100m from the salt base.

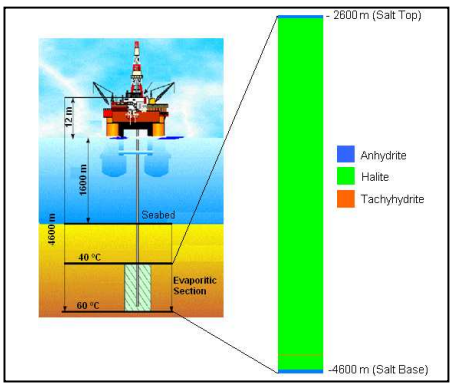

Fig. 20. Simplified Geological profile used in case study 1.

The temperature at the top of the salt interval is 40°C and at the base 60°C. The well will be drilled with a diameter of 17 ½" and a 14" casing will be used.

The axisymmetric model, according to the longitudinal axis of the well, comprises 2000m of salt rocks and 200m of thick hard rock, above and below the anhydrite layer to represent the boundary condition. 86418 quadratic isoparametric elements (with 8 nodes) and 264063 nodal points are employed in the finite element model, as shown in Figure 21.

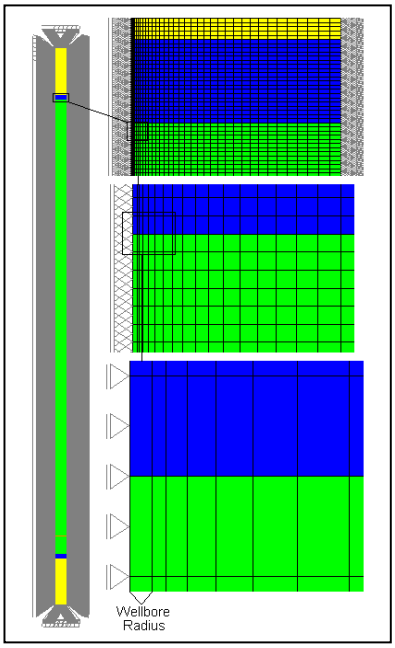

Fig. 21. Finite element mesh, axisymmetric model (Case 1).

To consider the temperature variation and the lithology in depth, different layers were built. As it was used the constants isolated in creep tests at the temperature of 86ºC, it is necessary to correct the creep constants by the thermal activation factor ($\exp^{(Q/RT_0 - Q/RT)}$).

The hard rocks with fragile behavior, above and below the salt, are analyzed according to an elasto/plastic model; it being adopted the Mohr-Coulomb plastic flow criteria for the multiaxial state of stresses. During the plastic flow is considered the isotropic behavior, with associative law of plasticity [17]. For the lithostatic column the average specific weight of 22.56kN/m^3 is used. Table 1 summarizes the elastic properties [22].

Table 1. Elastic constants for the materials

Material	E(kPa)x10^7	ν
Halite	2.040	0.36
Carnallite	0.402	0.36
Tachyhydrite	0.492	0.33
Fine Limestone	3.100	0.30
Cement	2.100	0.25
Casing	21.000	0.28

Numerical prediction of well closure: drilling fluid design

Numerical simulations were performed to predict the evolution of the well closure with time during drilling the salt interval, along its longitudinal axis, during the progress of the drilling column. To simulate the structural behavior of the well it is adopted the strategy of drilling the full salt interval in just one stage. It is considered that salt layers were drilled in excavation steps, simulating the bit progress in 10m/h.

Figure 22 shows the evolution of the 17 ½" well closure with time, when it is adopted from 11 lb/gl to 14 lb/gl mud weight. As is expected, the tachyhydrite layer has a very high closure rate, and the halite layer, a low closure rate.

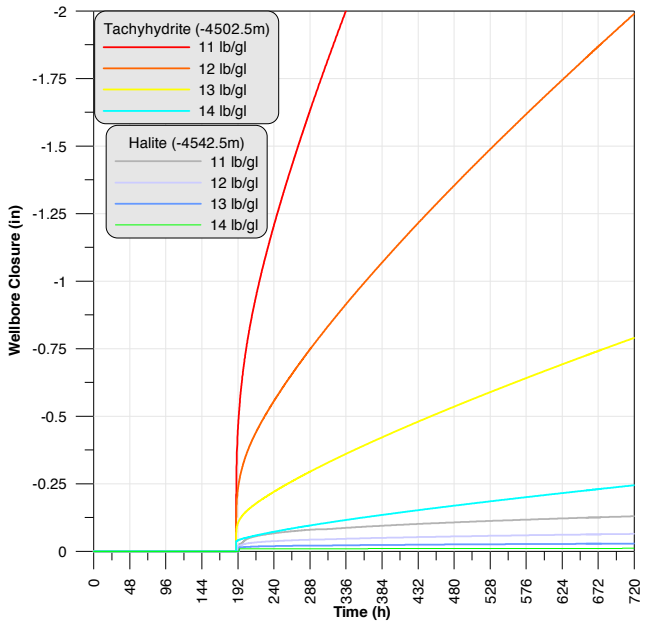

Fig. 22. Closure curves with 11, 12, 13 and 14lb/gl mud weight in 2 different depths along the axis of the well.

Considering a minimum thickness of 0.75" for the cementation of the 14" casing, for a well 17 ½" in diameter, the acceptable closure will be 2". The curves of well closure with time of each depth begin when the bit reaches the respective depth. For example, notice that the curve of well closure in the depth of -4502.5m, in a tachyhydrite layer, with 11lb/gl mud weight begins around the instant t = 192h, in which the bit reaches the respective depth. The well closure in that depth reaches the acceptable value around the instant t = 336h, about 144h after the bit has reached the respective depth. It is concluded that the drilling fluid weight of 11lb/gl is not able to keep the well open for enough time to complete the drilling operation without the risk of stuck pipe. At the same time, the well would not be open long enough for the casing set.

In this case in order to have enough time to complete the drilling operation and set the casing, use a drilling fluid over 12lb/gl is recommended.

The backreaming process, beneficial to the well, as it brings back the original well diameter, releases the deviating stress and reduces the creep behavior of the salt rocks, was not simulated in this case study.

7.2. Case Study 2

The prospect expected 300m of different salt rocks, to be drilled at the interval of 5700m to 6000m, (WD = 1600 m), Figure 23. The well will be drilled with a diameter of 12 1/4" and a 9 5/8" casing will be used. The temperature at the top of the salt interval is 140°C and at the base 150°C.

In this case, even though the thickness of the salt interval is lower, which would make drilling easier, the larger overburden and higher temperature, would directly influence on the higher rate of creep flow of salts in the existing range.

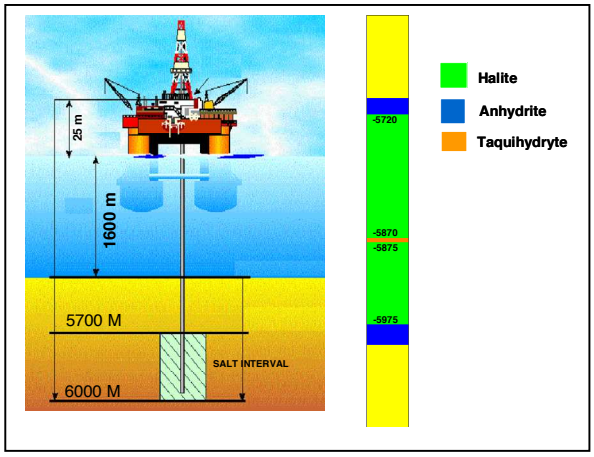

Fig. 23. Simplified Geological profile used in the case study 2.

The axisymmetric model, according to the longitudinal axis of the well, comprises 300m of salt rocks and 200m of thick hard rock, below and above the salt interval to represent the boundary condition. 5500 quadratic isoparametric elements (with 8 nodes) and 17523 nodal points are employed in the finite element model, as shown in Fig. 24.

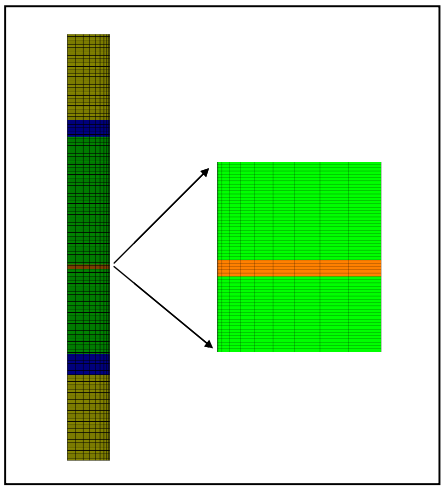

Fig. 24. Finite element mesh, axisymmetric model (Case 2).

Figure 25 shows the evolution of the well closure with time in the middle of the tachyhydrite layer for four different drilling fluids, from 12 lb/gl to 15lb/gl. It is clear that for a drilling fluid of 12lb/gl, the well closes completely in few hours in the tachyhydrite intercalation. In this case in order to have enough time to complete the drilling operation and set the casing, use a drilling fluid of 15lb/gl is recommended.

The main effect caused by the very high closure rate of the well is the large overburden on the salt interval and high temperature.

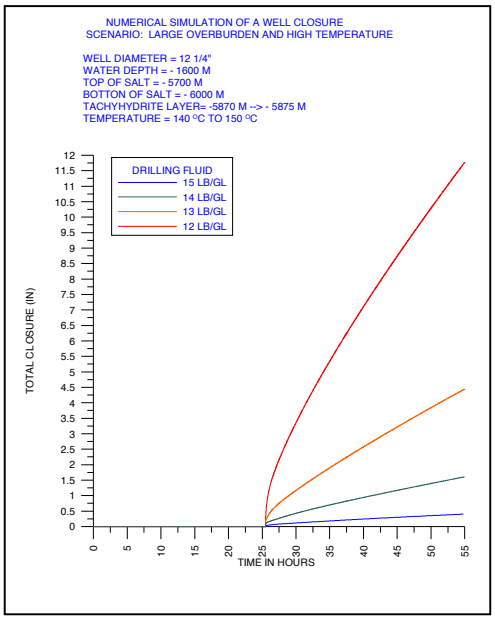

Fig. 25. Closure curves in the middle of the tachyhydrite layer with 11, 12, 13 and 14lb/gl mud weight.

8. FINITE ELEMENT MODEL OF THE CASING DESIGN FOR CASE STUDY 1

The casing design was accomplished with several cementation failure scenarios, from 5-20% uncemented, in the annulus casing/borehole through the salt layer. The aim is to determine the effect of non-uniform loading induced by salt creep on well casing deformation [24].

The computer codes used for pre and post processing and for the numerical simulations of the finite element model are the same used in the well closure simulation.

The plane strain model, perpendicular to the longitudinal axis of the well was built with 14506 quadratic isoparametric elements (with 8 nodes) and 43639 nodal points in the finite element model, Fig. 26. The depth analyzed was in a tachyhydrite layer.

The model diameter was build with 100m, sufficient to avoid the boundary effects (borehole 17 ½"), with boundary fixed ends. The modeling consist in two steps: first the mesh rezone (excavation) is applied in a circular well with symmetrical closure. After a specific time the casing and cement was introduced, with the rebuild process developed in ANVEC program.

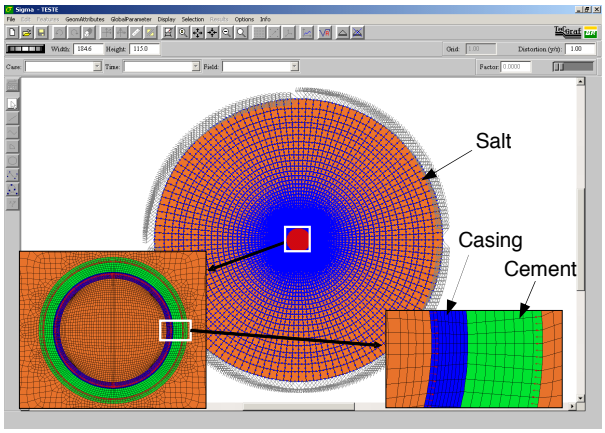

Fig. 26. Finite element model, plane strain model.

8.1. Numerical simulation of casing design

Numerical simulations were performed to predict the salt loading on well casing induced by the salt creep. The casing was designed to be capable of supporting tachyhydrite high creep rate.

Figure 27 shows the results in the numerical model with a 100% cemented annulus, after 500h in a concentric well. The stress in the high collapse casing (14"x 0.722" – P110 -9500psi – 1.5% maximum ovalization) is just 0.23 of SMYS, due to the uniform loading.

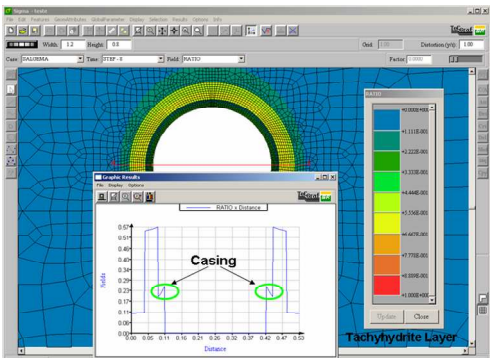

Fig. 27. 100% cemented annulus, after 500h in a concentric wellbore.

In deep-set casing through the salt layers, it is probable that the salt/casing annulus will remain uncemented. Simulations were done to evaluate 5%, 10%, 15% and 20% of cement channeling after 500h, Figs 28a-d respectively. From 15% cement channeling, the casing collapse is induced by the non-uniform loading.

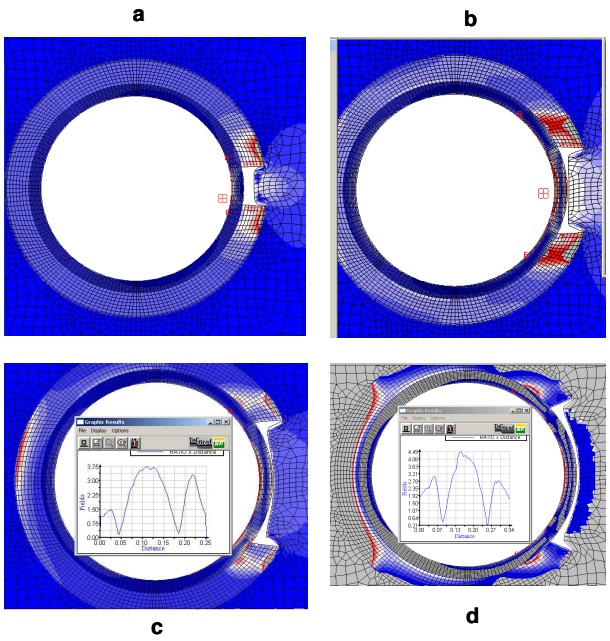

Fig. 28. Cement channeling a) 5%, b)10%, c)15% and d)20%.

To avoid the loading points in the casing caused by the cement channeling, in this case study, at least 90% cementation is necessary. To guarantee this index, a short job cementation is recommended, and this way is possible a deep-set casing in front of tachyhydrite.

To minimize this, a dense mud (16.6lb/gl) is simulated, placed between the top of the cement shoe and the casing head, rebuild the drilling fluid instead the cement in the simulation. This fluid redistributes the loads uniformly. The pressure increase in the shoe, created by the closure of the hole, is 818 psi in 490h and the radial casing deformation is 7E-3m and the stress in the casing is 0.57 of SMYS, Figure 29. The same analysis was performed, but the casing is considered non-concentric, Figure 30. The stress in the casing reaches 0.61 of SMYS, only 4% higher than the concentric case.

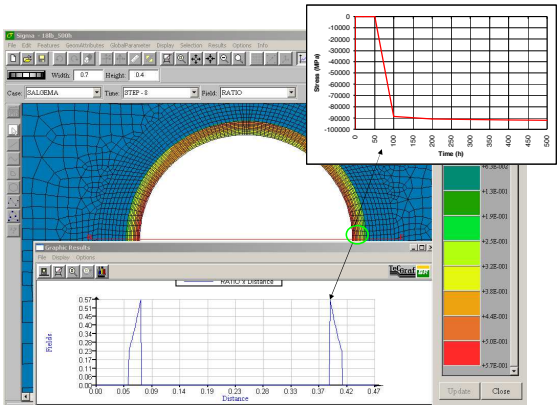

Fig. 29. Dense mud (16.6lb/gl) placed in annulus salt/casing concentric.

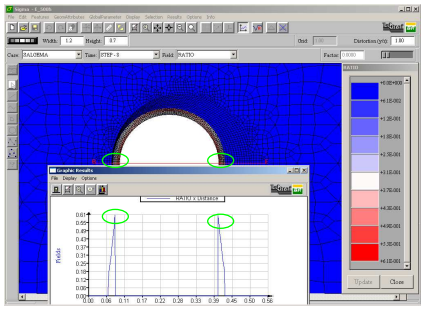

Fig. 30. Dense mud (16.6lb/gl) placed in annulus salt/casing non-concentric.

9. CONCLUSIONS & RECOMMENDATIONS

- This work presents a methodology developed by Petrobras for mud weight and casing design and also to define the strategy for drilling sub salt prospects.
- 2D and 3D computer modeling to evaluate the creep behavior of salt rocks subjected to high differential stress and high temperature and casing loads due to salt creep was applied.
- The numerical simulations have been done through the application of an in-house developed computer code based on the finite element method.
- The mud weight through the salt is more dependent on the temperature and state of stress than on the salt thickness. Drilling through thinner salt layers subjected to a larger overburden and higher temperature, is more difficult than drilling through shallow thick salt layers.
- In the casing design through the salt layers is important to analyze cement failure scenarios in

order to guarantee the well integrity during the well life.

- Employing the Seismic While Drilling to determine the base of the salt, to set the casing just above the expected rubble zone, and therefore, preventing loss of circulation is a good strategy.
- Foresee the salt type (halite, carnallite, tachyhydrite) present in the well facilitates adoption of a strategy that avoids stability problems and reduces the risk of losing the well.

REFERENCES

1. Oliveira, J.E. and L.S. Idagawa, E.C. Nogueira. 1985. *Evaporite in Campos basin: geological aspects and drilling problems*. Rio de Janeiro: PETROBRAS.
2. Modica, C.F. and R.H. Brus. June 2004. Postrift sequence stratigraphy, paleogeography, and fill history of the deepwater santos basin, offshore southeast Brazil. *AAPG Bulletin*. 88: 7, 923-945.
3. Barker, J.W. and W.R. Meeks. 2003. Estimating fracture gradients in gulf of mexico deepwater, shallow, massive salt sections. In *Proceedings of the SPE Annual Technical Conference and Exhibition, Denver, Colorado, 5 – 8 October, 2003*.
4. Falcao, J.L. 2001. Drilling in high-temperature areas in brazil: a wellbore stability approach. In *Proceedings of the SPE Latin American and Caribbean Petroleum Engineering Conference, Buenos Aires, Argentina, 25 – 28 March, 2001*.
5. Barker, J.W., K.W. Feland, and Y.H. Tsao. 1992. Drilling long salt sections along the U.S. Gulf Coast. In *Proceedings of the SPE Annual Technical Conference and Exhibition, Washington, DC, 4 – 7 October, 1992*.
6. Amaral, C.S., A.M. Costa, C.J.C. Gonçalves, and C.F Fonseca. 1999. *Reavaliação do comportamento do poço 1-rjs-480 por ocasião do fechamento do revestimento de 95/8 no Trecho de Travessia da Zona de Sal"*. Rio de Janeiro: PETROBRAS.
7. Munson, D.E., A.F. Fossum, and P.E. Senseny. 1990. Approach to first principles model prediction of measured wipp (Waste Isolation Pilot Plant) in-situ room closure in salt. *Tunneling and Underground Space Technology* 5, 135.
8. Munson, D.E. and K.L Devries. 1991. Development and validation of a predictive technology for creep closure of underground rooms in salt. In *Proceedings of the Seventh International Congress on Rock Mechanics, Deutschland, 7 - 1991*.
9. Frayne, M.A. and D. Z.: Mraz. 1991. Calibration of a numerical model for different potash Ores. In *Proceedings of the Seventh International Congress on Rock Mechanics, Deutschland, 7 – 1991*.
10. Costa A.M., E.J. Poiate, J.L. Falcão, C.O. Cardoso, and R.S. Rocha. 2003. *Previsão numérica do comportamento do poço 1-RJS-602 durante a travessia da zona de sal e dimensionamento do fluido de perfuração*. Rio de Janeiro: PETROBRAS.
11. Costa A.M. and E.J. Poiate. 2003. *Previsão numérica do comportamento do poço lua norte 1-RJS-601 durante a travessia da zona de sal e dimensionamento do fluido de perfuração*. Rio de Janeiro: PETROBRAS.
12. Poiate E.J., A.M. Costa, and R.B. Garske. 2004. *Acompanhamento de testemunhagens de carnalita do poço 7-CP-1498-SE*. Rio de Janeiro: PETROBRAS.
13. Poiate E.J., A.M. Costa, and R.B. Garske. 2004. *Acompanhamento de testemunhagens de taquidrita do poço 7-SZ-433-SE*. Rio de Janeiro: PETROBRAS.
14. Costa A.M. and E.J. Poiate. 2003. *Acompanhamento dos ensaios de fluência sobre amostras de rocha halita – Projeto 600102 - período de julho a outubro de 2002*. Rio de Janeiro: PETROBRAS.
15. Costa A.M., E.J. Poiate, and J.L. Falcão. 2005. Triaxial creep tests in salt applied in drilling through thick salt layers in Campos Basin-Brazil. In *Proceedings of the SPE Annual Drilling Conference, Amsterdam*.
16. Amaral C.S., A.M. Costa, M.T.M. Carvalho, and W.W.M. Lira. 1996. *Descrição do sistema SIGMA – sistema integrado em geotecnia para múltiplas análises*. Rio de Janeiro: CENPES/PETROBRAS.
17. Costa, A.M. 1984. *Uma aplicação de métodos computacionais e princípios de mecânica das rochas no projeto e análise de escavações subterrâneas destinadas à mineração subterrânea*. Tese. Rio de Janerio: COPPE/UFRJ.
18. Costa, A.M., P.D. D'Elia, L.F.R. Moreira, and L.C. Coelho. 1990. *Estudo de mecânica das rochas e dimensionamento dos painéis de lavra da camada inferior de silvinita da mina de Sergipe*. Rio de Janeiro: PETROBRAS.
19. Costa, A.M. 1995. *Análise da influência da espessura de laje de silvinita e carnalita sobrejacente à taquidrita em inibir a fluência da taquidrita*. Rio de Janeiro: Vale do Rio Doce.
20. Costa, A.M. 1995. *Simulação do comportamento de fluência do painel D1 e câmara experimental C1D1, dimensionamento do painel de lavra para a camada inferior de silvinita da mina de potássio de Taquari-Vassouras-Sergipe*. Rio de Janeiro: Vale do Rio Doce.
21. Costa, A.M. 2000. *Reavaliação do comportamento do painel de lavra i4a da mina de potássio de Taquari-Vassouras*. Rio de Janeiro: Vale do Rio Doce.
22. Filho, V.M. and A.M. Costa. 1985. A técnica de sísmica de transmissão direta na obtenção de parâmetros elásticos de maciços rochosos com aplicação em projetos de escavações subterrâneas. In *Proceedings of the Second Underground Meeting, Rio de Janeiro/Brazil, 1985*.
23. Fredrich, J.T., D. Coblentz, A.F. Fossum, and B.J. Thorne. 2003. Stress perturbations adjacent to salt bodies in the deepwater Gulf of México. In

Proceedings of the SPE Annual Technical Conference and Exhibition, Denver, Colorado, 5 – 8 October, 2003.

24. Willson S.M., A.F. Fossum, and J.T. Fredrich. 2002. Assessment of salt loading on well casings. In *Proceedings of the SPE Annual Drilling Conference, Dallas, Texas, 26 – 28 February, 2002*.

25. Costa, A.M. and C. Fairhurst. 1985. Comparison of numerical modelling with predictions from lab: tests & field observations of deformations in a potash mine in Sergipe Brazil. In *Proceedings of the U.S. Symposium on Rock Mechanics, June, 1985*.

26. Poiate Jr, E., Costa, A. and Falcão, J., 2006. Well design for drilling through thick evaporite layers in Santos Basin – Brazil. In *Proceedings of the IADC/SPE Drilling Conference, Miami, Florida*.

27. Costa, A. M. and Poiate Junior, E., 2008. Rocha salina na indústria do petróleo: aspectos relacionados à reologia e à perfuração de rochas salinas. In Mohriak, W.; Szatmari, P.; Anjos, S. M. C. *SAL*: geologia e tectônica. São Paulo: Editora Beca. cap. 17.

28. Costa, A.M.; D'Elia, P.C.; Coelho, L.C.; Ebecken, N.F.F.; Queiroz, J.L. 1991. Rock mechanics and computational methods applied to the design of the postah mine in Brazil. In *International Work-shop - Applications of Computational Mechanics in Geotechinical Engineering, Rio de Janeiro, 29 – 31 July 2001*.

NOMENCLATURE

E =Young's Modulus (MPa)

h = hour

in = inch

ISRM = International Society for Rock Mechanics

K = thermal conductivity (BTU/(°F.ft.h))

n = Stress exponent of salt rocks

Q = activation energy = 12 kcal/mol

R = Universal gas constant = 1.9858E-03 kcal/mol.K

SMYS = Specified Minimum Yield Strength = 758MPa

T = Temperature of rock (K)

T_0 = Reference temperature (K)

ε = Strain rate due to creep at the steady state condition

ε_0 = Reference strain rate due to creep (in steady state)

ρ = density (lb/gl)

ν = Poisson's Ratio

σ_{ef} =Creep effective stress

σ_0 = Reference effective stress

SI METRIC CONVERSION FACTORS

ft x 3.048	E–01 = m
lb/gl x 1.298264	E+02 = kg/m^3
psi x 6.894757	E+00 = kPa
in x 2.54	E–02 = m